Colloid & Polymer Science Colloid & Polymer Sci. **260**, 1023–1028 (1982)

COLLOID SCIENCE

Attractive interactions in critical scattering from non-ionic micelles

J. B. Hayter and M. Zulauf

Institut Laue-Langevin, Grenoble, France and
European Molecular Biology Laboratory, Grenoble Outstation, Grenoble, France

Abstract: We have studied the temperature-dependent critical scattering of both light and neutrons from aqueous solutions of *n*-octyl pentaoxyethylene glycol monoether (C_8E_5). We show that the assumption of a short-ranged temperature-dependent attractive pair potential between approximately spherical micelles of constant size permits a quantitative analysis of the neutron scattering data. The analysis, which is undertaken using current liquid-state theory and is in analytic form, contains only one free parameter, the depth of the attractive potential. We find that a potential with a range of only a fraction of a nm is sufficient to generate spatial correlations over tens of nm as the attractive potential deepens on approaching the critical temperature. The analysis also provides a semi-quantitative understanding of the light scattering data as a function of concentration and temperature, and leads to a qualitative prediction of the form of the phase diagram. Numerical values obtained are consistent with the hypothesis that the primary effect of raising the temperature is to lower the degree of structure of water near the micelle surface, allowing increased van der Waals attraction due to closer contact.

Key words: Micelles, critical scattering, attractive potential, neutron scattering, light scattering.

1. Introduction

Non-ionic detergents with polyoxyethylene head groups [1] form aqueous micellar solutions which exhibit a critical demixing phenomenon when the solution temperature is increased to a value T_d, the lower consolution temperature giving rise to a cloud point at a given detergent concentration [2–4]. As this temperature is approached, the intensity of forward-scattered radiation (light, x-ray or neutron) and the apparent hydrodynamic radii determined by photon correlation spectroscopy diverge following power-laws in the reduced temperature $(T_d-T)/T_d$ [5, 6]. The critical region where such laws hold extends over some tens of degrees below T_d [6], which is typically of order 300–350 K. In the past, light scattering measurements on these systems have often been interpreted in terms of micellar growth, the assumption being that micellar weight increases as T_d is approached [2, 7–9]. Indirect evidence from NMR spin-lattice relaxation [10] and dye solubilization [2] does not, however, support this hypothesis. An alternative explanation for the light scattering results is to assume that the micelles maintain constant size and (approximately spherical) shape as the temperature is raised, but that critical concentration fluctuations arise due to increasingly attractive intermicellar interactions as T_d is approached [4–6]. Recent neutron and light scattering experiments [11] have shown that this interpretation is consistent with measured data for the system *n*-octyl pentaoxyethylene glycol monoether (C_8E_5) in water.

In this paper we present evidence which strongly supports the idea that attractive interactions between spherical micelles of constant size play a primordial rôle in the critical behaviour of these non-ionic systems. In particular, we furnish a quantitative explanation of neutron scattering data from C_8E_5 micelles as a function of temperature on the basis of a single parameter, the depth of the (short-ranged) attractive potential near the micelle surface. The method of analysis, which is in a convenient analytic form, also allows a semi-quantitative understanding of the variation of the intensity of forward-scattered light as a

function of concentration at each temperature. The values obtained for the depth of the potential minimum indicate that the physical origin of the attraction may involve structured water near the micelle surface. As the temperature is raised, this structure is weakened, allowing increased van der Waals attraction due to the possibility of closer contact between micelles and leading to strong spatial correlations.

2. Experimental

Solutions of C_8E_5 (*n*-octyl pentaoxyethylene glycol monoether; BACHEM, Switzerland) were prepared in D_2O for both neutron and light scattering experiments. The lower consolution temperatures, determined from cloud-point measurements, were found to be slightly lower than in H_2O (for the phase diagram, see [11]); at 7% v/v, for example, T_d was found to be 329.7 K, which is 2.8 K lower than in H_2O. Light scattering measurements were performed as described in [11]. Both static and dynamic neutron scattering measurements were performed on the neutron spin-echo spectrometer IN11 at the Institut Laue-Langevin [12], using experimental conditions detailed in [13]. A solution concentration of 7% v/v was used for all temperature dependent neutron measurements; this concentration, which yields the minimum value of T_d, was chosen to correspond to previous studies [6, 11]. Static intensity data was normalized to scattering from H_2O under the same experimental conditions when absolute scaling was required. All data was taken at an incident neutron wavelength $\lambda = 0.83$ nm and was corrected for incoherent background, absorption and solvent scattering. Scattering angles 2θ were in the range $1.5 < 2\theta/\text{deg} < 20$, corresponding to a range of momentum transfer of $0.2 < Q/\text{nm}^{-1} < 2.6$ ($Q = (4\pi/\lambda)\sin\theta$).

3. Results and discussion

3.1 Neutron scattering

The static neutron scattering data shown in figure 1 exhibits the typical divergence of the forward-scattered ($Q = 0$) intensity observed as the critical temperature is approached. Under the assumption that the micelles are spherical (or nearly so) and relatively monodisperse in size, the observed coherent intensity per micelle may be factored [13, 14]:

$$I(Q) = P(Q)\,S(Q). \qquad (1)$$

Here, $P(Q)$ is the scattering function for a single micelle (governed solely by micelle geometry in a given solvent) and $S(Q)$ is the intermicellar structure factor (calculable from modern liquid-state theory [15]) describing the correlations between the positions of micelle centres. Noting that any such structure factor oscillates about unity and is damped fairly quickly as a function of Q, the figure allows two important conclusions to be drawn. Firstly, the coincidence of the data at high Q implies that $P(Q)$ remains constant as a function of temperature, since $S(Q) \approx 1$ in this Q-range. Secondly, since $P(Q)$ is found to be independent of temperature, the divergence of $I(O)$ is due to the divergence of $S(O)$ alone; that is, it is driven by a change in the intermicellar correlations, rather than resulting from a change in micelle shape or size.

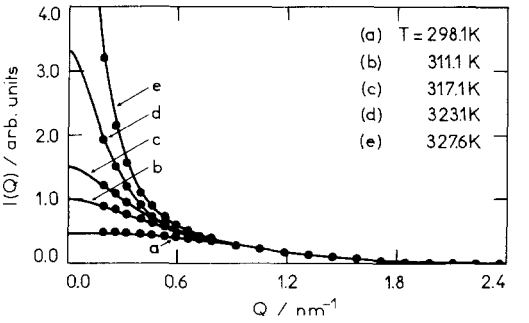

Fig. 1. Scattered neutron intensity $I(Q)$ as a function of momentum transfer Q for a 7% v/v solution of C_8E_5 in D_2O at the temperatures indicated. Fits to (1) are shown as solid lines (see text)

The behaviour of $P(Q)$ for $Q > 0.6\ \text{nm}^{-1}$ indicates a micelle diameter of $\sigma = 4.7 \pm 0.3$ nm. This data alone, however, cannot unambiguously exclude elongated micelles since in the latter case only the smallest dimension will influence $P(Q)$ in this Q range. We have therefore also used dynamic neutron spin-echo measurements [12, 13] of the effective diffusion coefficient to obtain an independent estimate of the micelle geometry. These dynamic measurements, which are reported elsewhere [11], are consistent with spherical micelles having the diameter obtained from $P(Q)$. That geometry has therefore been retained for all calculations which follow. From the corresponding micelle volume and known geometry of C_8E_5, we are able to estimate an aggregation number ν of about 77 ± 8 on the basis of two-shell packing (hydrocarbon core plus hydrated polar head group layer), taking about 6 solvent molecules per headgroup in the outer shell. (An aggregation number of about this magnitude of course follows immediately from taking a reasonable value for the micelle density (see e.g. [11]), independently of any model of packing). This type of model, which is discussed in detail in [13, 14, 16], allows the calculation of $P(Q)$ over the whole Q range of measurement, so that comparison of (1) with the measured data at each temperature provides values of $S(Q)$ which may be compared with a suitable model for the latter. This we obtain as follows.

We first note that the non-ionic system is stable due to steric interactions at temperatures well below T_d.

Since increased repulsive interaction will further depress $S(O)$ [17], we assume the observed increase in $S(O)$ at higher temperatures is related to an increasingly attractive force between micelles. Now the long-range asymptotic $(1/r^6)$ van der Waals potential is invariant under conditions of constant micelle size, and a significant change in the attraction between the neutral micelles is thus likely to be short-ranged. Noting that correlations between neutral microemulsion droplets are well described by excluded volume ("hard sphere") considerations alone [18], we therefore model the intermicellar pair potential $U(r)$ as hard-sphere plus a short-ranged attractive tail, taken of Yukawa form for mathematical convenience:

$$\begin{aligned} U(r) &= U_o \exp[-k(x-1)]/x, & x > 1 \\ &= \infty & x < 1. \end{aligned} \qquad (2)$$

Here, $x = r/\sigma$ where σ is the micelle diameter, $k = \varkappa\sigma$ where $\varkappa^{-1}$ is the range of the potential, and U_o is the depth of the attractive potential well.

For a potential of the form (2), $S(Q)$ has recently been calculated from liquid-state theory in closed analytic form as a function of U_o, k and the volume fraction $\phi = \pi n\sigma^3/6$, where n is the number density [17, 19]. Considering the short-ranged nature of the attraction, we have taken a fixed value of $\varkappa^{-1} =$ 0.3 nm, for reasons to be discussed below. All other parameters are then calculable from the micelle geometry and the concentration of C_8E_5 relative to the critical micellar concentration (cmc), so that (1) may be fitted to the measured data as a function of a single parameter, U_o. Fitted curves are shown as solid lines in figure 1; the micelle geometry described earlier was taken as fixed at all temperatures. Parameter values obtained were $U_o/k_BT = -2.5$ at $T = 298.1$ K, -6.4 (311.1 K), -8.5 (317.1 K), -11.8 (323.1 K) and -14.4 (327.6 K).

3.1.1 Origin of attraction

We may now consider the possible physical origins of the attraction. At very small interparticle separations, the van der Waals attractive energy between particles of the size considered here rises significantly above thermal energies. Since the system is stable at ambient temperature, such close contacts between micelles must be hindered by a barrier which becomes progressively weaker as the temperature is raised, allowing more frequent sampling of the strong van der Waals attraction; at T_d the barrier has become sufficiently weakened to allow collapse of the system. Considering the nature of the polyoxyethylene headgroup layer, a reasonable explanation for the origin of such a barrier is the presence of at least a monolayer of highly structured water at each micelle surface. As the temperature is raised, this structure will tend to "melt", allowing intermicellar contact to become more probable. We may formulate this idea on a more quantitative basis by estimating the van der Waals potential from Hamaker theory [20]:

$$\begin{aligned} U_{vw}(y) = &-(A/3)[1/(y^2 + 4y) \\ &+ 1/(y^2 + 4y + 4) \\ &+ 1/2 \log[(y^2 + 4y)/(y^2 + 4y + 4)]] \end{aligned} \qquad (3)$$

where $y = 2(x-1)$ is the surface-to-surface separation expressed in terms of the particle radius. Taking a reasonable minimum value of the Hamaker constant of $A = 5.5 \times 10^{-20}$ J [21], we find U_{vw} is of the order $-k_BT$ at a surface-to-surface separation of about 0.75 nm. At closer distances the attraction rises rapidly: $-4.6\ k_BT$ at 0.3 nm and $-11.9\ k_BT$ at 0.15 nm. These values are comparable with the values of U_o obtained from fits to the neutron data, and should also be compared with typical hydrogen bond energies of order 25 kJ mol^{-1}, or about 10 k_BT at ambient temperature. The distances involved are of order a hydrogen bond length, and justify *a posteriori* our choice of $\varkappa^{-1} \approx 0.3$ nm as the range of the attractive potential.

This idea that the phase transition is driven simply by the "melting" of structured water around the micelle as the temperature increases also allows a qualitative explanation of the dependence of T_d on the choice of surfactant and solvent (H_2O or D_2O). As the hydrocarbon chain length increases, the van der Waals attraction at a given separation increases with the micelle size and a lower value of T_d would be expected; increasing the polyoxyethylene length should increase the water structure and hence raise T_d. Both of these features are observed [22]. The lowering of T_d when D_2O is used in place of H_2O is seen to be a reflection of the fact that D_2O loses structure relatively faster than H_2O as the temperature is raised above room temperature, as evidenced by the smaller liquid range (m.pt. 277 K, b.pt. 374.5 K) and higher maximum density temperature (284.3 K) of D_2O.

3.1.2 Spatial correlation lengths

The values of U_o obtained from the fits to the data of figure 1, together with micelle geometry and con-

centration, allow calculation of $S(Q)$ over a wider range of momentum transfer than was employed in the experiments. The radial distribution function $g(r)$, which measures the probability of finding a neighbour at a distance r from a given micelle, may then be determined by a Fourier transformation [17]. Considering first $S(Q)$, figure 2 shows that only the long-wavelength (compressibility) limit of the structure factor [15] varies significantly with increasing depth of the shortranged attractive potential. At higher Q, the fairly quickly damped oscillations remain in phase, only increasing in amplitude very slightly compared with the dramatic increase of $S(O)$. These features correspond to the development of the well-defined real-space correlations which are evident in the radial distribution functions shown in figure 3. Recalling that the probability of finding a neighbour in a spherical shell situated between radii r and $r+dr$ from a given micelle is $4\pi r^2 g(r)dr$, the figure shows that correlated neighbours are increasingly likely to be found at a large distance as the temperature is raised. At temperatures well below T_d, the initial effect of a temperature increase is to augment the probability of

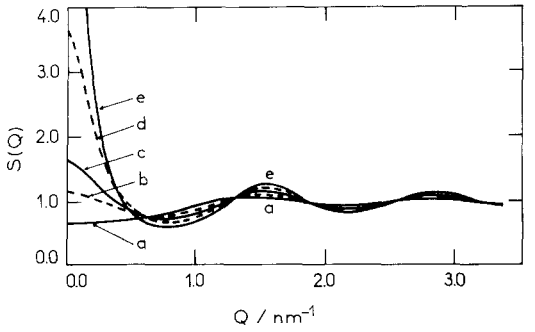

Fig. 2. Theoretical intermicellar structure factors $S(Q)$ calculated using parameters obtained from the fits to the data of figure 1, to which the labels (a)–(e) correspond

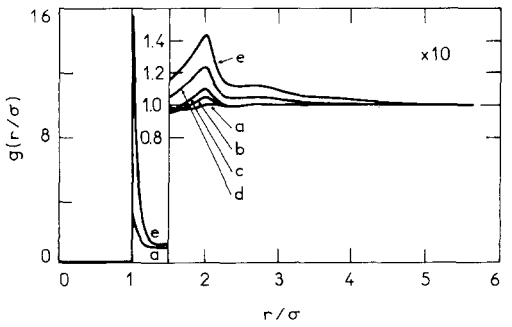

Fig. 3. Radial distribution functions $g(r)$ calculated by Fourier transformation of the data of figure 2, to which the labels (a)–(e) correspond. Note that the distance scale is measured in terms of the micelle diameter σ

contact, $g(r=\sigma)$. As the temperature is raised further, a second-neighbour peak develops at a distance of two diameters, indicating that chains are starting to form. Finally, as T_d is approached, other neighbours are added at increasing distances. There is now a less well-developed likelihood of higher neighbours being at an exact multiple of the particle diameter; this reflects the fact that bent chains or clusters are more probable than a linear chain, once several micelles are involved. The correlation lengths which develop may be estimated from figure 3. At the highest temperature (T_d – 2 K, curve e), $g(r)$ is still significantly different from unity at four diameters from the reference particle. Taking σ = 4.7 nm, this indicates correlation lengths already of the order of 20 nm at a temperature 2 K below T_d.

3.2. *Light scattering*

For particles of the size considered in this study (σ = 4.7 nm), light is scattered with essentially zero momentum transfer relative to the inverse particle size. We have measured the forward-scattered intensity, $I(O)$, relative to that scattered by the solvent, $I_w(O)$, as a function of surfactant concentration at different temperatures. The results (fig. 4) have been normalized approximately to scattering per micelle by dividing by the volume-fraction, ϕ_s, of micellized surfactant (calculated from the surfactant concentration in excess of the cmc). In the absence of micellar hydration, $\phi_s = \phi$; otherwise the two quantities are slightly different but proportional if a constant hydration number per micellized monomer is assumed. The experimental intensities $I(O)$ quoted are thus approximately given by

$$I(O) = CnV\,P(O)\,S(O)/\phi \qquad (4)$$

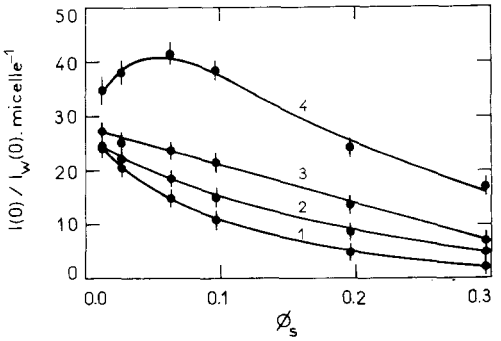

Fig. 4. Normalized forward scattered light intensity $I(O)/I_w(O)$ per micelle as a function of the micellized surfactant volume-fraction ϕ_s of C_8E_5 in D_2O. (1) T = 291.1 K, (2) 298.1 K, (3) 311.1 K, (4) 317.1 K. Solid lines are guides for the eye

where V is the volume of the sample and C is an experimental constant. Now $\phi = n\bar{v}$, where $\bar{v}$ is the volume per micelle, and for spherical micelles $P(O)$ is approximately proportional to $\bar{v}^2$. At a given volume-fraction, $I(O)$ is thus proportional to the product of $S(O)$ and the micelle volume. If we first assume that the micelle size is independent of volume-fraction (as well as independent of temperature), the analysis of the preceding section permits us to calculate the expected intensity variation directly from $S(O)$, using values of U_o obtained from the neutron data to set the temperature scale. Figure 5 shows $S(O)$ calculated as a function of ϕ for parameter values suitable for comparison with the light-scattering results of figure 4. At low temperatures, the relative intensity loss is predicted quantitatively ($U_o/k_BT = -2.5$ in fig. 5 corresponds to the temperature of curve 2 in fig. 4, for example).

At higher temperatures, this quantitative agreement is lost, but the qualitative features are still visible in $S(O)$, in particular the change in character of the functional form, which develops a peak. The peak position, however, is displaced relative to that of the data, and the latter decays faster than $S(O)$ as ϕ_s increases. The possible origins of this discrepancy may arise from our assumptions that both $P(O)$ and the potential parameters are independent of ϕ in calculating the values of figure 5. In the case of charged micelles, for example, micelle size is known to increase with volume-fraction in concentrated solution [13, 14, 16]. The latter effect, which increases $P(O)$, decreases $S(O)$ due to the range of the interaction becoming relatively smaller compared with the size of the micelle. We have also assumed that $\phi \approx \phi_s$, and that in calculating the latter the amount of free surfactant is equal to the cmc at all concentrations; neither condition may be strictly obeyed over the wide concentration range studied. The complexity of the interplay of these effects leads us to consider that at present a further quantitative analysis of figure 4 would not be fruitful. We have sufficient confidence in the qualitative theory, however, to present the more complete set of values of $S(O)$ shown in table 1, where constant micellar size has been assumed for the sake of example. The most interesting feature of this table is that it emulates the phase diagram of the system on the sole basis of changes in the intermicellar attraction at short range. At a given volume-fraction, increasing the attraction (which corresponds to raising the temperature) leads to a phase change, indicated by the divergence of $S(O)$. At higher volume-fractions, the temperature at which this occurs is lower, as observed [6, 11].

4. Conclusion

From static and dynamic neutron scattering measurements on C_8E_5 in 7% v/v solution (the concentration at which the temperature of demixing T_d is minimum) we conclude that the observed divergence of the forward-scattered intensity is due to the onset of long-ranged spatial correlations between approxi-

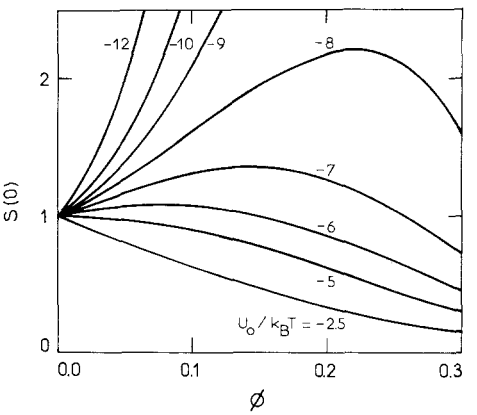

Fig. 5. The variation of $S(O)$ as a function of micelle volume-fraction ϕ, calculated at the values of U_o/k_BT shown on the curves. The micelle geometry and range of the potential have been taken as fixed (see text)

Table 1. Calculated values of $S(O)$ as a function of the depth U_o of the attractive potential at different micellar volume-fractions ϕ. The range of the potential ($\varkappa^{-1} = \sigma/16$) and the diameter σ have been assumed constant throughout the table

	U_o/k_BT								
ϕ	−2.5	−5	−6	−7	−8	−10	−12	−15	−20
0.01	0.96	1.00	1.02	1.03	1.05	1.08	1.12	1.18	1.29
0.05	0.80	0.98	1.06	1.16	1.27	1.56	1.96	2.93	7.79
0.10	0.62	0.90	1.07	1.30	1.61	2.73	5.80	∞	∞
0.15	0.46	0.77	1.00	1.35	1.95	5.91	∞		
0.20	0.33	0.61	0.85	1.27	2.18	35.8			
0.25	0.23	0.45	0.65	1.04	2.08	∞			
0.30	0.15	0.30	0.44	0.73	1.60				

mately spherical micelles of fixed size. We have shown that the assumption of a short-ranged temperature-dependent attractive pair potential between neighbouring micelles permits a quantitative analysis of the data on the basis of a single parameter, the depth U_0 of the potential. In particular, a potential having a range of only a fraction of a nm generates spatial correlations over several tens of nm as the critical temperature is approached, through chaining or clustering of the micelles. The calculation of the intermicellar structure from the pair potential, which is undertaken using modern liquid-state theory and involves no *ad hoc* assumptions from the point of view of statistical mechanics, is in a convenient analytic form which allows direct comparison with experiment. The values of U_0 are found to be of order the van der Waals energy at a surface-to-surface separation corresponding to one or two interposed water molecules. This leads us to argue that the increasing attraction as the temperature is raised corresponds primarily to a breakdown of water structure near the micelle surface, allowing more frequent sampling of the van der Waals potential at short distances. We emphasize, however, that the physical origin of the attraction has no bearing on our main conclusion, namely that the phase transition is driven by the onset of short-ranged attraction (of whatever origin) between micelles. Using this analysis we are also able to explain semi-quantitatively the dependence of scattered light intensity on surfactant concentration and temperature, and are able to predict the qualitative form of the phase diagram.

References

1. Examples are offered by alkyl POE (C_xE_y; Brij, Lubrol, AL), phenyl POE (Triton, Igepal, Nonidet), POE sorbitol esters (Tween, Emasol, Cemulsol), where POE = polyoxyethylene. An exception is octyl glucoside.
2. Herrmann, K. W., J. G. Brushmiller, W. L. Courchene, J. Phys. Chem. **70**, 2909 (1966).
3. Hall, D. G., B. A. Pethica, in: "Nonionic Surfactants", Vol. 1, ed. M. J. Schick (Marcel Dekker, New York, 1967).
4. Corti, M., V. Degiorgio, Opt. Commun. **14**, 358 (1975).
5. Corti, M., V. Degiorgio, J. Phys. Chem **85**, 1442 (1981).
6. Corti, M., V. Degiorgio, M. Zulauf, Phys. Rev. Lett. **48**, 1617 (1982).
7. Balmbra, R. R., J. S. Clunie, J. M. Corkill, J. F. Goodman, Trans. Faraday Soc. **58**, 1661 (1962); idem, **60**, 979 (1962).
8. Ottewill, R. H., C. C. Storer, T. Walker, Trans. Faraday Soc. **63**, 2796 (1967).
9. Tanford, C., "The Hydrophobic Effect", (Wiley, New York, 1980).
10. Staples, E. J., G. J. T. Tiddy, J. Chem. Soc. Faraday Trans. I, **74**, 2530 (1978).
11. Zulauf, M., J. P. Rosenbusch, J. Phys. Chem. (in press).
12. Hayter, J. B., in: "Scattering Techniques Applied to Supramolecular and Non-Equilibrium Systems", eds. S. H. Chen, B. Chu, R. Nossal, NATO ASI Series B, Vol. 73 (Plenum, New York, 1981).
13. Hayter, J. B., J. Penfold, J. Chem. Soc. Faraday Trans. I, **77**, 1851 (1981).
14. Hayter, J. B., J. Penfold, to be published.
15. Hansen, J. P., I. R. McDonald, "Theory of Simple Liquids" (Academic Press, London, 1976).
16. Hayter, J. B., T. Zemb, submitted to Chem. Phys. Letts.
17. Hayter, J. B., J. Penfold, Molec. Phys. **42**, 109 (1981).
18. Cebula, D. J., D. Y. Myers, R. H. Ottewill, Colloid and Polymer Sci. **260**, 96 (1982).
19. Hayter, J. B., J. P. Hansen, Institut Laue-Langevin Report 82HA14T (1982).
20. Van Megen, W., I. Snook, Faraday Disc. Chem. Soc. **65**, 92 (1978).
21. Mahanty, J., B. W. Ninham, "Dispersion Forces" (Academic Press, London, 1976).
22. We measured the following cloud point temperatures for 10% surfactant solutions in H_2O: C_8E_4: 313.8 K; C_8E_5: 332.9 K; $C_{12}E_5$: 304.8 K; $C_{12}E_6$: 323.9 K; $C_{12}E_7$: 336.8 K and $C_{12}E_8$: 349.7 K.

Received August 6, 1982;
accepted August 9, 1982

Authors' addresses:

J. B. Hayter
Institut Laue-Langevin
156X
38042 Grenoble Cedex, France

M. Zulauf
European Molecular Biology Laboratory
Grenoble Outstation
156X
38042 Grenoble Cedex, France